Finite size scaling of density of states in photonic bandgap crystals

Shakeeb Bin Hasan, Elahe Yeganegi, Allard P. Mosk, Ad Lagendijk, Willem Vos
Complex Photonic Systems (COPS), MESA+ Institute for Nanotechnology, University of Twente, P.O. Box 217, 7500 AE Enschede, The Netherlands
(Dated:)

The famous vanishing of the density of states (DOS) in a band gap, be it photonic or electronic, pertains to crystals in the infinite-size limit. In contrast, all experiments and applications pertain to finite crystals, which raises the question: Upon increasing the size L of a crystal, how fast does the DOS approach the infinite-crystal limit? Answering this question, however, requires an understanding of how linewidth of the modes in crystal with finite support scales as a function of crystal length L. We develop such a theory in a finite support crystal using Bloch-mode broadening due to the crystal boundaries. Our results suggest that total DOS inside a bandgap has the same scale dependence irrespective of the number of dimensions which the crystal is defined in. This can pave the way to establishing design rules for the usage of vanishing density of states, notably to cavity QED, quantum information processing, and Anderson localization.

arXiv:1701.01743v1 [physics.optics] 6 Jan 2017

The discovery brought about by crystallography that a crystal consists of an infinitely extended periodic array of basic units with perfect periodic symmetry [1] has led to the birth of modern condensed matter physics [2–4]. The quantum-mechanical description of the electronic degrees of freedom has led to the notion of density of states (DOS), and to the characterization of semiconductors as having a range of vanishing density of states, bandgap, with associated band edges [3, 4]. Remarkably, the most important observable - the electric conductance - is only defined for systems that deviate from perfect crystalline symmetry in that they have a finite size instead of infinite translational symmetry [2]. The size-dependence of the conductance is one of the pillars of condensed matter physics, and the study of finite-size scaling in general plays a central role in condensed matter and statistical physics [3, 5–7].

An analogy can be drawn between electronic condensed-matter and photonic condensed-matter phenomena, as the underlying mechanism is in both cases wave interference [3, 4]. Indeed photonic crystals reveal Bragg reflections for light, which are apparent as a beautiful iridescence [8]. When the light-matter interaction is sufficiently strong, photonic crystals can develop a bandgap analogous to electronic semiconductors and insulators [9–11]. The nanophotonic analogue of a semiconductor is widely considered to be a photonic crystal with a complete 3D band gap in the photonic DOS [9–11].

Most theories of the density of states in condensed matter and nanophotonics consider infinite samples ($L \to \infty$). Examples are the plane-wave expansion for wave states - both electronic [2] or photonic [11] - or the thermodynamic limit in liquid state theory [12], that all maximally exploit the underlying periodic or continuous symmetry. Theories for the density of states of waves, electrons and photons, that address a finite sample are rare [13]. To the best of our knowledge, there are no theories that address a sample with finite support, that is, a sample where a finite "crystal" is embedded in infinite free space. A potential with finite support implies the complication due to the presence of an interface.

The central concept of a bandgap, electronic or photonic [9, 10, 14], pertains to infinite systems only. In contrast, experiments and applications are obviously made with real and finite crystals [15, 16], which raises the question: How fast does the DOS in the band gap of a finite-crystal approach the infinite-crystal limit? In other words: what is the scaling behavior of the DOS? We attempt to address this problem in the following section by means of ab-initio calculations and phenomenological approach to describe the scaling of DOS a finite-support crystal.

We begin with a toy-model by considering a non-magnetic homogeneous, isotropic medium possessing permittivity ε which is real but less than zero. Such a medium does not possess any optical states since the real part of propagation constant is zero and thus serves as an analogue of a photonic bandgap crystal made up of non-absorbing media. To introduce the effect of finite support, we consider a sphere made up of such material and surrounded by vacuum. Hence, while the sphere itself does not afford any modes, the vacuum interface contrives to introduce optical states through evanescent tunnelling. The local density of states (LDOS) in such a geometry can be analytically solved [17] and we use it to calculate DOS inside the sphere according to

$$\rho_{\mathrm{sph}} = \frac{3}{a^3}\int_0^a dr r^2 \rho_{\mathrm{LDOS}}(r)\,. \tag{1}$$

Figure 1 plots the DOS inside the sphere ρ_{sph} normalized to that of vacuum (ρ_0) for a fixed frequency ($k_0 = \omega/c$) as a function of varying radius a. It is evident from Fig. 1(a) that DOS inside the sphere scales with $1/k_0a$ except for small values of k_0a which are highlighted in Fig. 1(b). The nonlinear behavior is due to the coupling of evanescent modes across the spherical interface for sufficiently smaller diameters ($2a$). Hence, once the diameter becomes large enough the ρ_{sph} assumes the

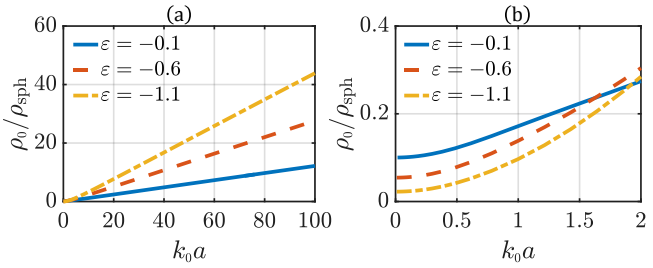

Figure 1: (a) DOS (normalized to vacuum) inside a sphere of permittivity $\varepsilon < 0$ as a function of radius a. (b) DOS inside the sphere for smaller radii when the relationship is not linear due to size being comparable with evanescent decay length of vacuum modes inside the sphere. The minimum value of $k_0 a$ in each plot is 0.01.

stable character of decaying inversely with $k_0 a$.

Extending a similar treatment to realistic photonic crystal geometries is not straightforward and even numerical calculations become prohibitively expensive, not to mention a lack of possibility to draw insight into the underlying physics. Therefore, we resort to a phenomenological model to describe modes sustained by a finite support photonic bandgap crystals. We consider the modes in a crystal with finite support to be Lorentzians characterized by resonance frequency $\omega_{n,\mathbf{k}}$ and linewidth $\Delta_{n,\mathbf{k}}$. The DOS $\rho(\omega)$ for a crystal of size $L^{\rm D}$ is then given as

$$\rho(\omega) = \frac{1}{(2\pi)^{\rm D}} \sum_n \int \mathbf{dk} F(\omega - \omega_{n,\mathbf{k}}, \Delta_{n,\mathbf{k}}), \qquad (2)$$

where D is dimensionality factor equal to the number of spatial dimensions, n the index of frequency band and $F(\omega - \omega_{n,\mathbf{k}}, \Delta_{n,\mathbf{k}})$ the Lorentzian function defined as

$$F(\omega - \omega_{n,\mathbf{k}}, \Delta_{n,\mathbf{k}}) \equiv \frac{1}{2\pi} \frac{\Delta_{n,\mathbf{k}}(L)}{(\Delta_{n,\mathbf{k}}(L)/2)^2 + (\omega - \omega_{n,\mathbf{k}})^2}. \qquad (3)$$

In the perfect crystal limit of $L \to \infty$, the modes become impulses and we retrieve the familiar expression for DOS

$$\lim_{L\to\infty} \rho(\omega) = \frac{1}{(2\pi)^{\rm D}} \sum_n \int \mathbf{dk} \delta(\omega - \omega_{n,\mathbf{k}}). \qquad (4)$$

Figures 2(a) and (b) schematically illustrates the model for the case of finite support and infinite crystals respectively. In order to proceed further, we need to make a few more approximations. To begin with, we consider the resonance frequency of the modes $\omega_{n,\mathbf{k}}$ to be determined completely by the Bloch propagation constant according to

$$|\mathbf{k}.\mathbf{L}| = m\pi, \qquad (5)$$

for some integer m from 0 to number of unit cells N and the length $\mathbf{L}$ which is considered as a vector to signify the direction dependence of length encountered by a

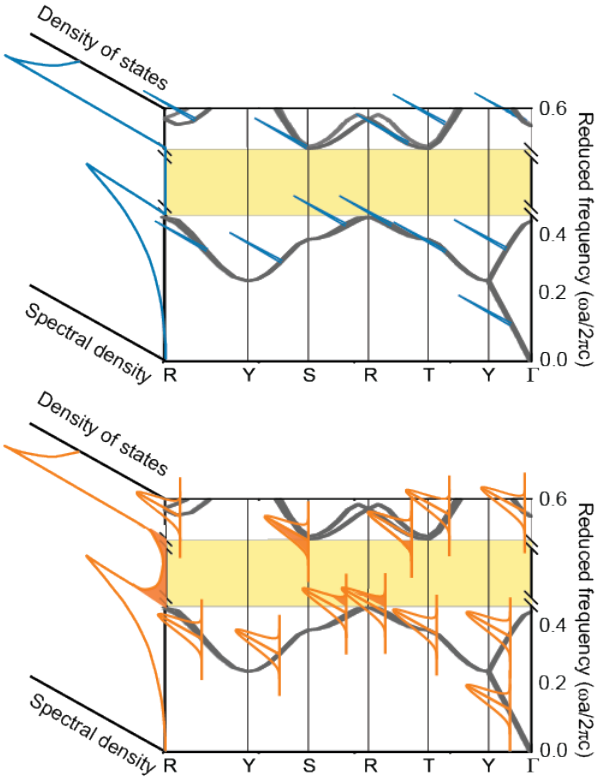

Figure 2: Schematic drawing of crystal modes that contribute to the DOS. (a) In an infinite 3D photonic crystal modes are delta functions (blue peaks) that only appear on bands outside the gap. The resulting density of states, plotted in the third dimension at the left, vanishes in the band gap and is only non-zero outside the gap. (b) In a finite crystal, the modes become Lorentzians (orange), with a number of modes equal to the number of unit cells. Since the modes have finite width, they extend into the band gap, leading to a non-zero density of states in the gap (orange-filled area).

Bloch mode along $\mathbf{k}$. Besides resonance, the linewidth of standing waves formed in a finite support crystal is given by

$$\Delta_{n,\mathbf{k}} = -\ln|r(\omega_{n,\mathbf{k}})| \frac{2|\mathbf{v}_g(\mathbf{k})|}{L}, \qquad (6)$$

where $r(\omega_{n,\mathbf{k}})$ is the modal reflection coefficient of the Bloch mode which in general depends upon geometry of the vacuum-crystal interface too. Once again we simplify our calculations by assuming that $\ln|r(\omega_{n,\mathbf{k}})| \approx -1$.

With this, we are in a position to solve for the DOS in Eq. (2). First we consider a 2D photonic crystal made of cylindrical array on a square lattice as shown in the inset of Fig. 3(a). We take the dielectric cylinders with permittivity $\varepsilon = 8.9$ and radius $R = 0.2a$, with a being the lattice constant. The background medium is considered to be vacuum. The dispersion for s-polarization (electric field out of the plane) along high symmetry directions of the irreducible Brillouin zone (IBZ) is shown in Fig. 3(a) calculated by an open-source code based on plane wave

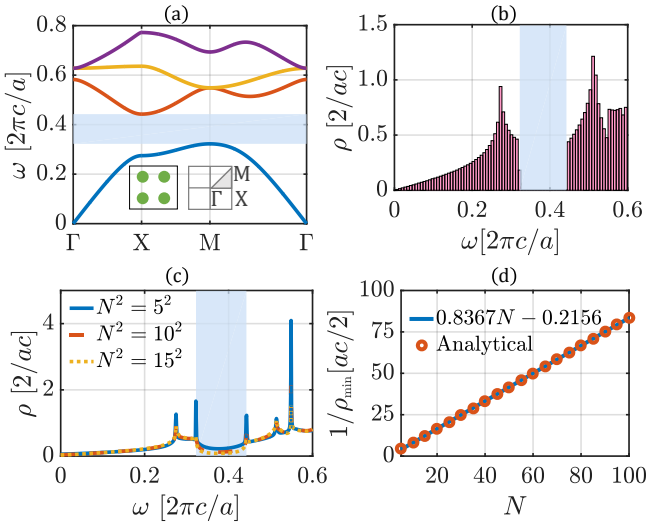

Figure 3: (a) Dispersion of the modes having electric field polarized out of the plane in a square lattice crystal of cylindrical array ($\varepsilon = 8.9$) in vacuum. Inset shows a schematic sketch of the unit cell and fundamental Brillouin zone. (b) DOS calculated for an infinite crystal by mode counting procedure. Size of frequency bins is $\Delta\omega = 0.001\,(2\pi c/a)$ while the IBZ was discretized with $\Delta k = 0.005\,(2\pi/a)$. (c) DOS calculated according to Eq. (2) for a crystal with finite support of area $L^2 = a^2N^2$, where N is the number of unit cells in each direction. (d) Minimum of DOS inside the bandgap as a function of the number of unit cells N in each direction. Solid blue curve is the linear fit while red circular marks represent DOS calculated using the semi-analytical approach of Eq. (2).

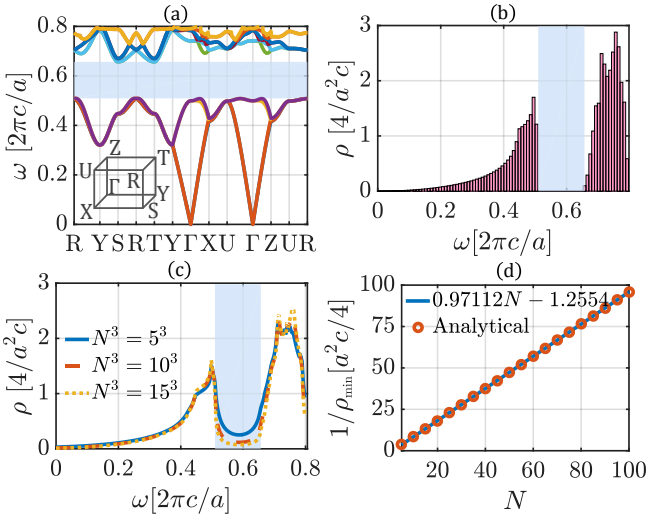

Figure 4: (a) Frequency dispersion along high symmetry directions of IBZ of an inverse woodpile crystal. The lattice constants of the two sides of orthorhombic cell is a while the third one is b with ratio $a/b = \sqrt{2}$. Air holes drilled into silicon ($\varepsilon = 12.1$) have a radius of $R = 0.24a$. Inset shows a schematic sketch of the IBZ of orthorhombic unit cell. (b) DOS calculated for an infinite crystal by mode counting procedure. Size of frequency bins is $\Delta\omega = 0.003\,(2\pi c/a)$ while the IBZ was discretized with $\Delta k = 0.02\,(2\pi/a)$. (c) DOS calculated according to Eq. (2) for crystal with finite support of volume $L^3 = a^2bN^3$, where N is the number of unit cells in each direction. (d) Minimum of DOS inside the bandgap as a function of the number of unit cells N in each direction with $N = 5$ as the minimum on horizontal axis. Solid blue curve is the linear fit while red circular marks is based on DOS calculations using semi-analytical approach of Eq. (2).

expansion method [18]. We find a bandgap of relative width $\Delta\omega =$ for the s-polarization of light. The corresponding DOS in an infinite crystal is shown in Fig. 3(b) obtained through calculating the dispersion of frequency bands in the IBZ discretized with $\Delta k = 1/200\,(2\pi/a)$ while the frequency bins for histograming the mode count was taken to be $\Delta\omega = 0.001\,(2\pi c/a)$. Naturally, the DOS vanishes inside the bandgap which is highlighted in blue. Now we calculate the DOS in a crystal with finite support of area $L^2 = N^2a^2$ which is shown in Fig. 3(c), where N is an integer denoting the number of unit cells. The sharp peaks observed in DOS are due to modes with small or vanishing group velocities. With infinite numerical precision this should of course become idealized delta peaks due to vanishing linewidth of the Lorentzian mode. However, with increasing crystal sizes, the corresponding grid size dk of the numerical integral in Eq. (2) decreases and in the limit of large crystal sizes (i.e. $dk \to 0$) all artificial peaks converge into well-defined density curves. This effect can already be seen in Fig. 2(c) for larger values of N^2.

To finally see the scaling of DOS, we plot the minimum of DOS inside the bandgap in Fig. 3(d). The calculated DOS from Eq. (2) is shown as circular marks while the solid blue curve represents a linear fit. It is curious to find linear decay of DOS which has already been observed for the 3D sphere considered earlier in Fig. 1. It should be pointed out that $N = 5$ is the minimum value on horizontal axis in Fig. 3(d). This cut-off limit, defined somewhat arbitrarily, was put in place in recognition of the fact that for sufficiently small crystals the Bloch mode description is not accurate anymore. That is why we ignore the negative DOS predicted for $N = 0$ by the linear fit in Fig. 3(d). In terms of the preceding example of a sphere, this pertains to the nonlinear regime shown in Fig. 1(b).

We now consider a 3D diamond-like inverse woodpile crystal which is known to exhibit a wide photonic bandgap [19, 20]. Figure 4(a) shows the dispersion along high symmetry directions (inset) of the crystal made up of silicon ($\varepsilon = 12.1$) with cylindrical air holes of radius $R = 0.24a$. The lattice constants of the orthorhombic unit cell have a mutual ratio of $a/c = \sqrt{2}$. The DOS sustained by the infinite crystal is plotted in Fig. 4(b) which is obtained by calculating dispersion in the volume of IBZ of the tetragonal unit cell discretized with $\Delta k = 0.02\,(2\pi/a)$ and histogrammed into frequency bins

equal to $\Delta\omega = 0.003\,(2\pi c/a)$. The corresponding DOS in a crystal with finite support of volume $V = N^3a^2b$, where N again is the number of unit cells in each direction, as shown in Fig. 4(c). Opting once again the frequency corresponding to minimum value of DOS inside the bandgap $[\omega = 0.59\,(2\pi c/a)]$, we plot it as a function of the number of unit cells N in Fig. 4(d). The circular red marks indicate the DOS calculated from Eq. (2) while the solid blue represents the linear fit. Quite intriguingly, we once again observe the same feature of linear decay as already observed in Fig. 3(d).

Remembering the exponential dependence of LDOS as a function of crystal size, the linear dependence of DOS regardless of the number of spatial dimensions defining the geometry might come as a surprise. However, it is possible to find a simple explanation for this behavior in crystals that are large enough to make Bloch mode description valid. In case of a photonic bandgap, the only electromagnetic states inside a finite support crystal are due to evanescent tunnelling of modes from the vacuum interface. When the crystal size is increased in discrete steps (i.e. by addition of complete unit cells), the geometry of vacuum-crystal interface remains the same and only enlarges in size. The increased size, therefore, corresponds to length of the interface for 2D crystals or area for the crystals defined in 3D space. For the spatial sum of modes inside the crystal $n\left(\omega, L^{\mathrm{D}}\right)$ we can write

$$n\left(\omega, L^{\mathrm{D}}\right) = \int \mathbf{dr}\rho_{\mathrm{LDOS}}\left(\mathbf{r}\right) \propto N^{\mathrm{D}-1}, \tag{7}$$

where D again is equal to the number of spatial dimensions and the integral runs only inside the crystal. However, DOS being a spatial average is obtained by normalizing the spatial sum of modes in Eq. (7) with area or volume of the crystal with finite support. Hence we get

$$\rho\left(\omega\right) = \frac{n\left(\omega, L^{\mathrm{D}}\right)}{L^{\mathrm{D}}} \propto \frac{1}{N}. \tag{8}$$

Therefore, if the crystal size $L^{\mathrm{D}} \propto N^{\mathrm{D}}$ is increased discretely with N, the proportionality constant should exhibit little sensitivity to increasing size since the geometry feature of the vacuum-crystal interface is unaffected. However, it would be a different matter if L^{D} is changed continuously then it should expectedly lead to periodic oscillations around the linear curves shown in Figs. (3) and 4(d).

To conclude, we presented a phenomenological approach to address the problem of the scaling of DOS in the photonic bandgap of finite support crystals. Our analysis revealed a linear decay of DOS inside the finite support structure when the crystal size is discretely increased by increasing the number of unit cells. Insights were also drawn into the problem by considering a toy-model of sphere which has an exact analytical solution and mimics finite support photonic bandgap crystals when the permittivity of sphere is negative.

This project is part of the research program of the Stichting voor Fundamenteel Onderzoek der Materie (FOM) FOM-program Stirring of Light!, which is part of the Nederlandse Organisatie voor Wetenschappelijk Onderzoe (NWO).

[1] W. H. Bragg and W. L. Bragg, Proceedings of the Royal Society of London A: Mathematical, Physical and Engineering Sciences **88**, 428 (1913), ISSN 0950-1207, http://rspa.royalsocietypublishing.org/content/88/605/428.full.pdf, URL http://rspa.royalsocietypublishing.org/content/88/605/428.

[2] N. Ashcroft and N. Mermin, *Solid state physics* (Saunders, 1976).

[3] P. Sheng, *Introduction to Wave Scattering, Localization and Mesoscopic Phenomena*, Springer Series in Materials Science (Springer Berlin Heidelberg, 2006), ISBN 9783540291565, URL https://books.google.nl/books?id=u7l4f65OnSUC.

[4] E. Akkermans and G. Montambaux, *Mesoscopic Physics of Electrons and Photons* (Cambridge University Press, 2011).

[5] P. W. Anderson, Phys. Rev. **109**, 1492 (1958), URL http://link.aps.org/doi/10.1103/PhysRev.109.1492.

[6] E. Abrahams, P. W. Anderson, D. C. Licciardello, and T. V. Ramakrishnan, Phys. Rev. Lett. **42**, 673 (1979), URL http://link.aps.org/doi/10.1103/PhysRevLett.42.673.

[7] M. E. Fisher and V. Privman, Phys. Rev. B **32**, 447 (1985), URL http://link.aps.org/doi/10.1103/PhysRevB.32.447.

[8] P. Vukusic and J. R. Sambles, Nature **424**, 852 (2003), ISSN 0028-0836, URL http://dx.doi.org/10.1038/nature01941.

[9] E. Yablonovitch, Phys. Rev. Lett. **58**, 2059 (1987), URL http://link.aps.org/doi/10.1103/PhysRevLett.58.2059.

[10] S. John, Phys. Rev. Lett. **58**, 2486 (1987), URL http://link.aps.org/doi/10.1103/PhysRevLett.58.2486.

[11] J. D. Joannopoulos, S. G. Johnson, J. N. Winn, and R. D. Meade, *Photonic Crystals: Molding the Flow of Light* (Princeton University Press, 2008).

[12] J.-P. Hansen and I. McDonald, *Theory of Simple Liquids* (Academic Press, 2013).

[13] F. Yndurain, J. Joannopoulos, M. L. Cohen, and L. Falicov, Solid State Commun. **15**, 617 (1974), ISSN 0038-1098, URL http://www.sciencedirect.com/science/article/pii/0038109874911569.

[14] V. Bykov, J. Exp. Theor. Phys. **35**, 269 (1972).

[15] S. Ogawa, M. Imada, S. Yoshimoto, M. Okano, and S. Noda, Science **305**, 227 (2004), ISSN 0036-8075, http://science.sciencemag.org/content/305/5681/227.full.pdf, URL http://science.sciencemag.org/content/305/5681/227.

[16] M. D. Leistikow, A. P. Mosk, E. Yeganegi, S. R. Huisman, A. Lagendijk, and W. L. Vos, Phys. Rev. Lett. **107**, 193903 (2011), URL http://link.aps.org/doi/10.1103/PhysRevLett.107.193903.

[17] H. Chew, The Journal of Chemical Physics **87**, 1355

(1987), URL http://scitation.aip.org/content/aip/journal/jcp/87/2/10.1063/1.453317.

[18] S. G. Johnson and J. D. Joannopoulos, Opt. Express **8**, 173 (2001), URL http://www.opticsexpress.org/abstract.cfm?URI=oe-8-3-173.

[19] K. Ho, C. Chan, C. Soukoulis, R. Biswas, and M. Sigalas, Solid State Communications **89**, 413 (1994), ISSN 0038-1098, URL http://www.sciencedirect.com/science/article/pii/003810989490202X.

[20] R. Hillebrand, S. Senz, W. Hergert, and U. Gösele, Journal of Applied Physics **94**, 2758 (2003), URL http://scitation.aip.org/content/aip/journal/jap/94/4/10.1063/1.1593796.